FNAL TD note TD-07-006
Oct. 2006 - Febr 2007. The final version of the note posted May 04, 2007

Focusing Solenoid HINS_CH_SOL_01
Fabrication Notes and Test Results

C. Hess, F. Lewis, D. Orris, M. Tartaglia, I Terechkine, T. Wokas

I. Fabrication Notes

This lens was built as a prototype focusing lens for the CH section of a HINS Front End linac. The main features of the solenoid have been described in the pre-release note TD-06-020 [1]. Certain changes in the design were made reflecting the use of a different strand in the main coil. Instead of the single-ML-coated SSC inner 0.808 mm strand made by IGC, double-Formvar-coated 0.8 mm strand was used. The insulated strand diameter was 0.84 mm (comparing to 0.826 mm in the previous case). The number of strand turns in the winding remained the same though: 2600.

Winding the main coil using the new strand was not as straightforward as it was in the case of the test coils. We still do not know the reason for this behavior, but it took many attempts and adjustments of winding parameters before the main coil was successfully wound in a regular pattern. The winding data for the main coil are:

- coil I.D. : 55.2 mm
- 26th layer O.D. @ 2586.37 turns: 95.4-95.5 mm
- 27th layer O.D. @ 2599.8 turns : 96.6-96.8 mm
- coil length at I.D. : 85.7 mm
- coil length at O.D. : 85.9-86.0 mm

Because the last layer was not fully filled with turns of the strand, for the magnetic field calculation, it was important to know the adjusted outer diameter of the coil:

OD_adj = 95.5 + 20.15/26*14/100 = 95.61 mm

For the length of the coil we use the average value: L = 85.8 mm. The compaction factor with these winding data becomes 0.754, which is quite close to what the coil wound using IGC strand showed, and is higher than the value assumed (0.71) in the preliminary magnetic design [1].

Bucking coils were wound using Oxford 0.6 mm strand. The length of the coils was 6.3 mm instead of 6.5 mm. In combination with the new winding data of the main coil, this change would prohibit getting the needed field profile. So, more turns (400 instead of 370) were wound in the bucking coils accompanied by somewhat reduced thickness of interlayer insulation. The rest of the bucking coil geometrical parameters are shown in the table below:

Coil	BC #1	BC #2
ID	53.18 mm	53.22
OD	99.9 mm	99.5 mm
L	6.3 mm	6.3 mm
Compaction Factor	0.768	0.776

Although it was planned to leave a gap of ~0.2 mm between the flux return body and the flux return flange, to compensate for core contraction during cool down (see [2]), this feature was not implemented during the first assembly of the device (by mistake, it was

not reflected on the assembly drawing). Also, as a result of this error, the flux return was not positioned symmetrically against the coil assembly.

The rest of the assembly went fine, including pre-compression of the coil assembly by stretching the beam pipe and subsequent welding it to the flux return. The final assembly features are shown in Fig. 1 below.

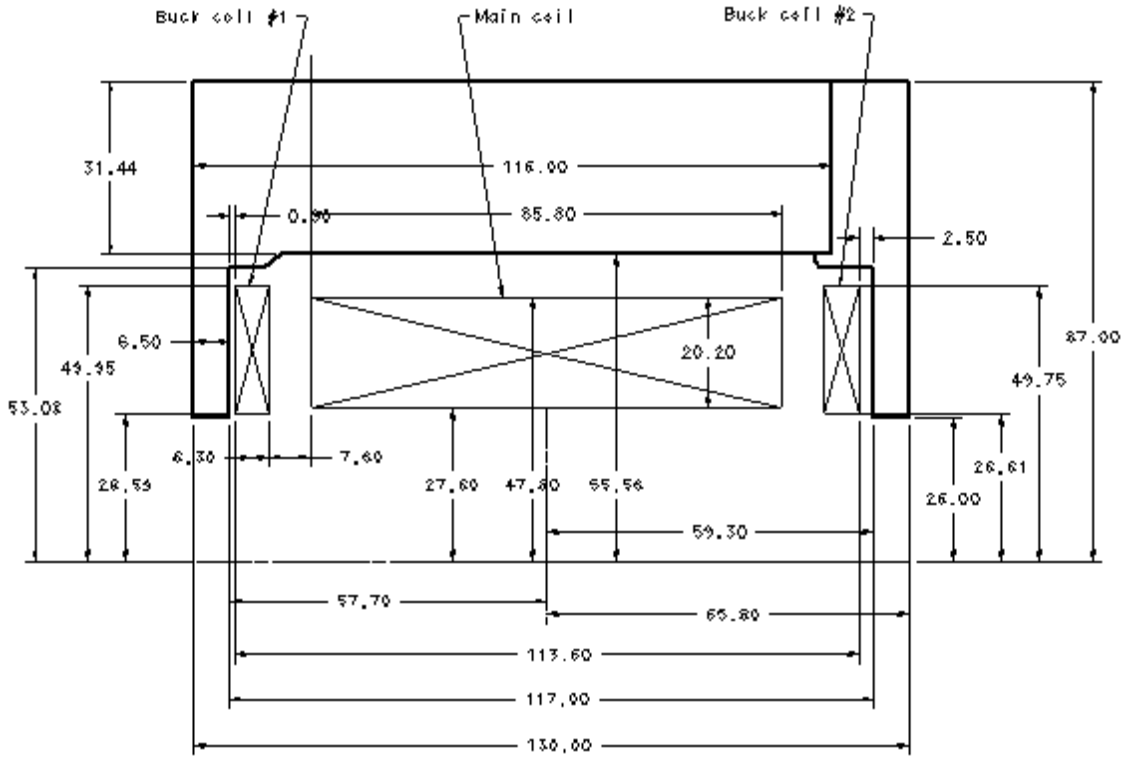

Fig. 1: HINS_CH_SOL_01 as built

To find the solenoid quench characteristics, we need to know the strand critical surface: for the 0.6 mm strand used to fabricate the bucking coils, this surface was measured in the TD Short Sample Test Facility (SSTF) by E. Barzi and D. Turrioni and is defined by table 1 below. For the 0.8 mm main coil strand we did not have any test data during the first test; we relied instead on data supplied by the vendor (Oxford) shown in table 2 below.

Table 1: Critical current versus magnetic field for 0.6 mm strand, from SSTF lab

B (T)	0	1	2	3	4	5	6	7	8
I (A)	978	722	546	457	392	334	275	210	140

Table 2: Critical current versus magnetic field for 0.8 mm strand, from Oxford

B (T)	5	6	7	8
I (A)	555	443	332	220

The quench behavior of the lens can be determined from Fig. 2, where, for the main coil and bucking coil #1 (which has the highest magnetic field of the two bucking coils), the coil load lines intersect corresponding strand critical surfaces. The main coil working point is slightly higher than for bucking coil #1. For bucking coil # 2, the field in the gap

between the main and the bucking coil is a bit lower due to the fact that the system is not perfectly symmetrical, as it was mentioned earlier. The maximal current is 245 A, which is slightly lower than it was found in the pre-release note. See later for correction of this data made after 0.8 mm strand parameters were measured.

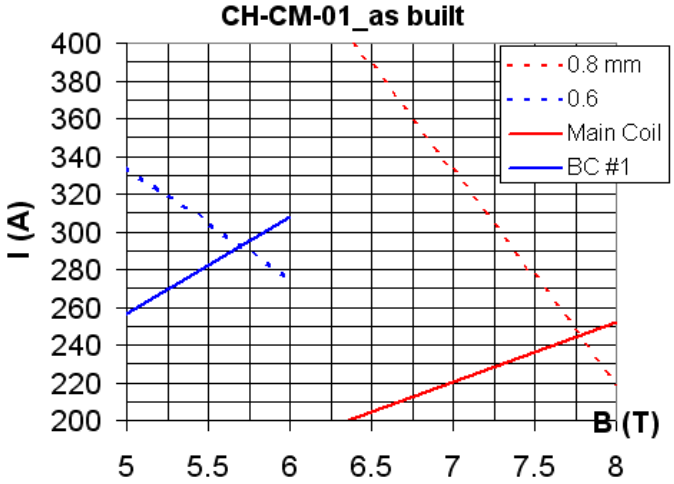

Fig. 2: Predicted quench performance of the coils at 4.2 K, for individually powered main coil (red) and bucking coil #1 (blue).

The effective length of the solenoid is 80 mm. This is a bit less than for the nominal design, which means that the magnetic field screening is also a bit better than the design goal (due to higher packing factor in the main coil). The calculated longitudinal field distribution on the side of the bucking coil #1 is shown in Fig. 3, starting outside of the cold mass (Z = 75). At the location of the first accelerating gap of the CH cavity one can expect a magnetic field of ~ 50 G. At the maximal current (245 A), the squared field integral along Z axis is 2.92 T^2m (compared to 3.14 T^2m in the pre-release note).

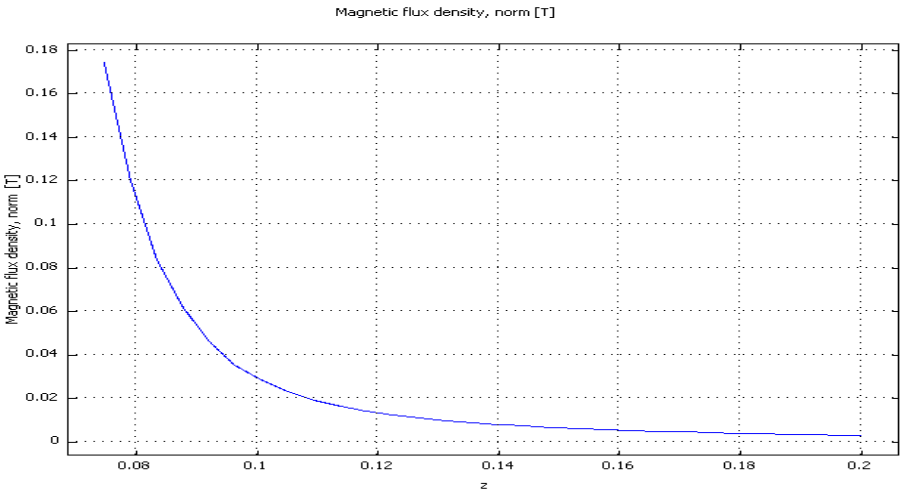

Fig. 3: Predicted magnetic field on the axis outside the solenoid

For configuring a protection system, it is important to know inductances of the main coil and the bucking coils. These were estimated, using handbook formulas, to be:
Lmain = 0.26 H, and Lbuck = 0.016 H.

II. Quench Protection and Data Analysis

This solenoid was tested three times. In this note we will present relevant data from all the three tests. During the first test, voltage readings from characterization voltage taps on the coils could not be interpreted properly because (as it was later determined) the polarities of several signals were inverted; so a correct conclusion about quench location could not be made ***during the test***. It was suggested at the time that the power system trips during current up-ramps were caused by voltage spikes due to a) relative motion of bucking coil relative to the main coil, or b) movement of inadequately supported strands in the splice region. Slight increases of the trip current resulted from increases in the quench detection threshold.

After voltage tap signal polarities were carefully checked, re-interpretation of the voltage signals led to the conclusion that quenches during the first test occurred in bucking coils and training was very slow. In an attempt to find a cure for the problem, the lens was taken apart and re-assembled with a modified pre-compression scheme that left a gap between the parts of the flux return (thus limiting free movement of bucking coils after cooling down and excitation) and with a revised splicing scheme that avoided making splices in areas with high field.

The lens was successfully retested after this work was complete; in fact, adequate liquid helium was available to perform a thermal cycle to room temperature and back to 4.3 K, where the lens quenched at the same current without re-training.

Finally, the tested cold mass was enclosed in a LHe vessel and was successfully re-tested in the same LHe Dewar, but in a horizontal orientation that models quite well the final assembly.

The quench protection system was designed to quickly switch off the power supply, and capture diagnostic voltage and current data, when any of the voltages across certain elements of the circuit exceed their corresponding threshold values. In the first test of this lens, the signals used for quench protection included all of the standard possibilities, for Sc and Cu lead protection, the difference of two “half coil” voltages, and the whole coil voltage. However, in later tests of the rebuilt magnet with fewer voltage taps, we relied simply on the whole coil signal to detect a resistive voltage growth. This resulted in an interesting and important lesson during the final test of the lens in its helium vessel: ***the whole coil voltage signal was inadvertently disconnected*** during the cold hi-pot procedure, ***therefore quench protection was not active*** when the magnet was powered. After the second such occurrence, we realized what had happened (and eventually determined how and why): when a quench occurred, the power supply quickly reached it’s maximum voltage as the coil resistance grew to about 27 Ohms, which forced the current to about 8 Amperes for a couple of minutes until we manually tripped the power supply off and captured voltage characterization data. Approximately 220 Watts of heat had very effectively boiled away the available liquid helium and the test was postponed until more helium was procured. Nevertheless, the lens subsequently performed well – fortunately the solenoids are self-protecting as long as the power supply voltage is properly limited (and the magnet is kept immersed in liquid helium).

Original Device Test

The study of quench performance was a primary goal in the original build of this device, which was the very first bucked solenoid lens. Quench training was conducted at

low ramp rates of 2 A/s or 1 A/s. The interpretation of quench data from the first test was initially confusing, but was later resolved by the realization (and demonstration) that signal polarities had not been correct. Shown below are voltage traces from a representative quench event of this device, which was labeled "fsch-p01" (focusing solenoid for CH section, prototype 01) before a device naming convention was fully accepted. The electrical circuit diagram in Figure 4 identifies positions of voltage taps available during the first test. While interpreting the graphs, it is important to know that polarities of all the signals are reversed except for the whole coil (WC voltage corresponds to T2/B4 potential difference). Also a dump resistor, R_d = 0.6 Ohm, was normally switched in series to the circuit at the time of quench detection (with no delay).

In the event shown in Figures 5 and 6, quenching started very early, at ~ 100 A. This early start was associated with possible movement in parts of the lens. Observed peaks on some voltage taps gave us this idea, which was strengthen by zero observed "whole coil" voltage. As a result of post-analysis, we came to a conclusion that the most probably we saw quenching BC #1, that was wound on a bobbin with copper flanges (BC #2 coil had G-10 flanges).

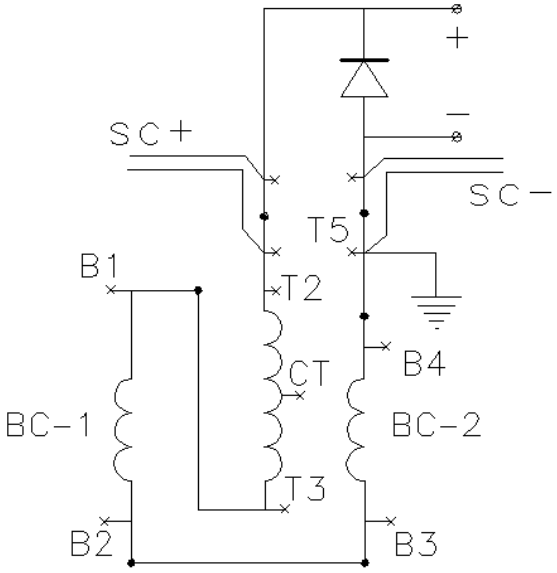

Fig. 4: Position of voltage taps during test of FSCH-P01 (original build of the lens later known as HINS_CH_SOL_01).

Mixed in with the quench training studies for this first solenoid was a measurement of the **splice resistances**. The voltage across three splices were measured at zero current, 50A, and 100A, with a NIST calibrated HP3458 (bar code 1107) set up to integrate over 40 power line cycles. The splice voltage taps T3-B1 (splice 1), B2-B3 (splice 2), and B4-T5 (splice 3) had been separately wired and brought out to make this measurement. The resulting resistance values were found to be 10, 5, and 4 micro-Ohms for splices 1, 2, and 3 respectively. These resistances were considered to be quite good for single strand splices.

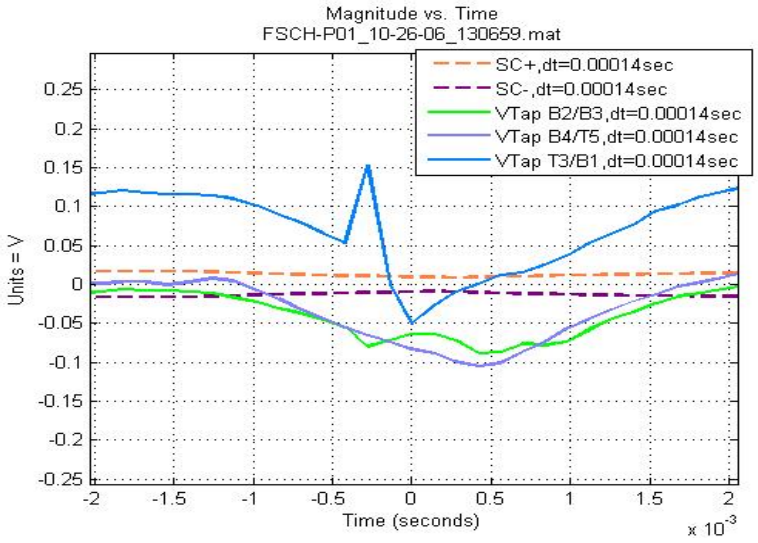

Fig. 5: Observed peak preceding trip event

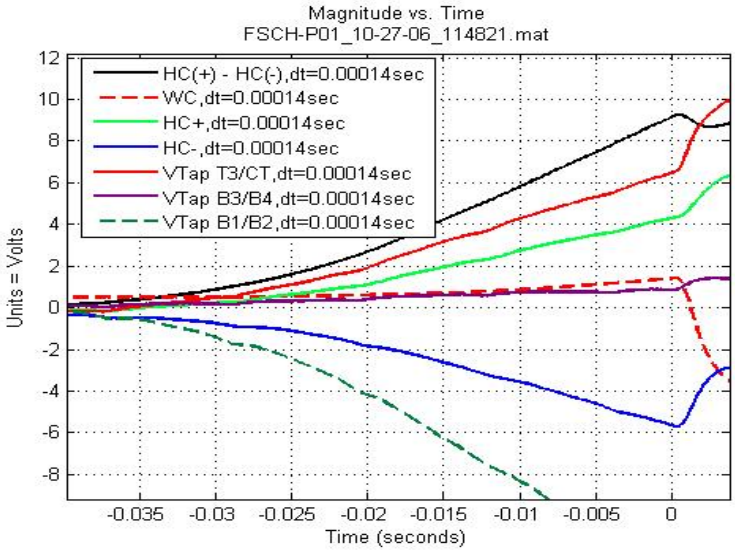

Fig. 6: Graph showing controversial polarities of the observed voltage tap signals

Rebuilt Device Test

During the second assembly, the axial compression force was increased up to 4000 N and a gap between the flux return and the flux return flange of 0.25 mm was left before the welding. This gap was completely closed after the welding, indicating that the pre-stress has increased beyond 4000 N. New data for the 0.8 mm Oxford strand became available (courtesy of E. Barzi and D. Turrioni). The new strand data table is shown below. Analysis of quench conditions with the new strand data gave an updated quench current of ~255 A and the maximum magnetic field on the winding of ~ 8.1 T (compare with 7.75 T in Fig. 2).

Table 3: Critical current data for 0.8 mm Oxford strand, from SSTF lab

B (T)	5	6	7	8	9
I (A)	664	531	398	260	115

The solenoid was tested again after reassembly. This time a provision was made to test the main coil and the bucking coils separately before making the final test of all coils powered in series. Again, training ramps were all performed at 2 A/s or less.

The stand-alone bucking coil test showed some training. The first quench was in the BC #1 (voltage taps T5 – CT/BC) at 161 A. The rest of the quenches were in the coil #2 (voltage taps CT/BC – T6) at the current values 211, 250, 257, 261, and 237 Amperes. After the last quench, the current reached 276 A without quenching (our safe power supply limit). The theoretical limit for the bucking coils is about 300 A, but further increase of the current was considered unnecessary taking into account that retraining is probable with the main coil also powered.

The stand-alone main coil also experienced some training. The coil quenched only once at 235 A before reaching a plateau value of ~ 246 A. The theoretical limit for the main coil alone is 240 A.

After the main coil and the bucking coils were connected in series, some retraining also took place. First, a series of BC #1 (voltage taps T5 – CT/BC) quenches occurred at the current levels of 172.5, 196.5, 233.5, 240.0 and 252.0 Amperes. Finally, the main coil quenched at 257.5 A and then (at lower ramp rate) at 258.0 A. Theoretical quench limit for the assembled system is 255 A, so performance of the solenoid was in good agreement with the prediction. An adequate helium supply allowed for a warm up to room temperature and second cool down to 4.3 K to check quench performance following a thermal cycle: the lens with all coils powered remembered its training, and quenched at 257.2 A.

Cryostat Assembly Test

The lens was subsequently assembled into a helium vessel, the next step in preparing the magnet for mounting into a separate cryostat. This required welding to flanges and thus potentially could influence quench performance by changing mechanical dimensions or internal stresses. The assembly was installed in the test stand 3 cryostat in a horizontal orientation. Splices to connect the main and the bucking coil were made inside the LHe vessel before welding (outside the high field region), so the complete lens was trained during this test.

As we highlighted at the start of the quench performance section, the test of this lens ran into difficulties with helium use and the quench protection system. First, the test was delayed almost one week after LHe arrived, so about 25% of LHe was lost before the test started. Second, the coil voltage taps were not connected to the quench protection system, and did not detect two quenches. After manually triggering and saving data, we found, at 8 A current, a signal of 27 V between the voltage taps T9 – T10 (BC #2 in Fig. 4). The resulting rapid boil-off of LHe forced us to stop the test and order additional LHe.

After the problem with protection circuit was fixed, the lens did not require any training to reach (and exceed) the same quench current level achieved before welding: 259A → 260A → 252A (4 A/s) → 256A (4 A/s) → 252A (4 A/s). The last three quenches occurred after performing several five-minute endurance tests at a plateau current of 255 A; for these, current ramp down rates of 4 A/s had been programmed, and is the likely cause of the quenches that occurred just after the plateau. When the ramp down rate was changed to 2 A/s, same as the current ramp up rate, no quench occurred.

III. Magnetic Measurements

As discussed earlier, the original assembly of this lens did not exhibit good quench performance, so the magnet was later re-assembled with the same components in a more stable mechanical configuration and with splices positioned in low field regions. For all tests, the measurement system made use of the same Hall probes, support and drive systems, and readout devices that were utilized for previous test solenoid measurements, shown in Table 4, with Labview readout of the probe voltages and positions. Precision Unix readout of magnet currents was not available in the first device cold test in October 2006, so the (less accurate) Labview values were recorded; in subsequent tests this Unix signal was available. The Labview current was found to be about 1% higher than the Unix value.

Table 4. Hall Probes and Digitizing Instruments

Probe Label	Probe Ser.No/ Bar Code	Instrument	Instrument Ser.No/Bar Code	Field Orientation wrt solenoid axis
A	BC 000833	Group3 DMT-141	BC 000801	1D, Parallel
B	BC 000811	Group3 DMT-141	BC 000801	1D, Transverse
C	SN 26-05	Keithley 2700	SN 899874	3D “old”
D	SN 54-06	Keithley 2700	SN 899874	3D “new”

In testing the original lens, the bucking and main coils were all connected in series, and rather extensive magnetic measurements were made at warm and cold temperatures using both 1D and 3D probes. These consisted mostly of “Z” scans to measure field strength versus position along the solenoid axis. Some measurements of field strength versus angle, at large radius (.51cm), were attempted at two different z positions; however, we observed erratic noisy behavior with the 3D probes, and did not come to any useful conclusion in this effort with regard to ability to determine the lens center position. Measurement results for the original device are shown in Figures 7-12. A slight constant offset (-0.0031 T) in the 1D probe strength, from having forgotten to zero the instrument before starting measurements, has been subtracted. The peak transfer function is found to be about 2 to 3% higher than the predicted value, and the field outside the coil appears to be attenuated more efficiently than predicted.

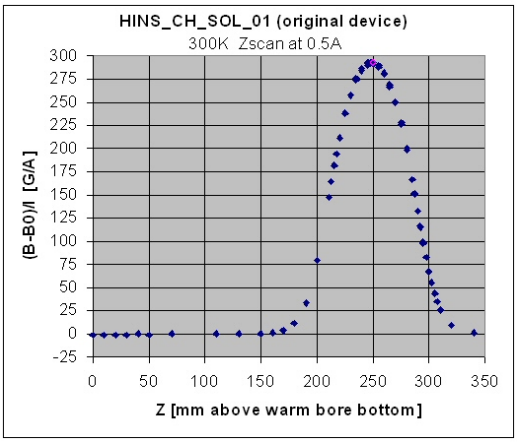

Figure 7. Field strength profile (normalized by current) along the solenoid axis, measured warm with 1D probe A.

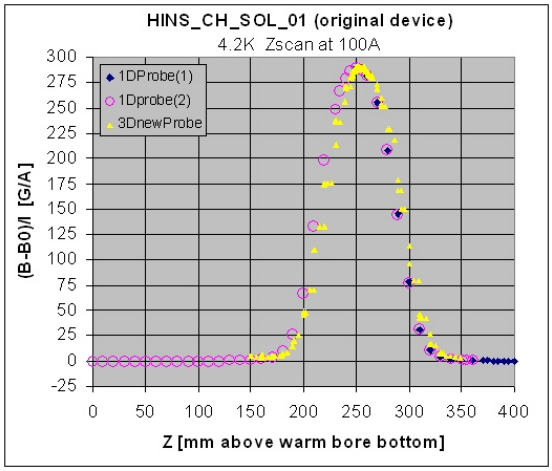

Figure 8. Field strength (normalized by current) along the solenoid axis measured cold. Two separate scans using the 1D probe A illustrate very good reproducibility; the 3D probe C is slightly offset in position due to differences in the probe supports.

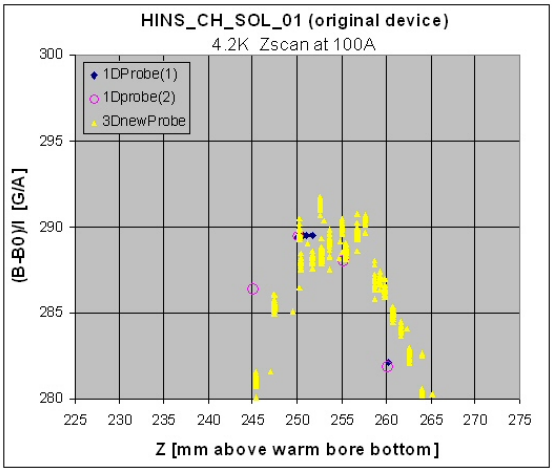

Figure 9. Peak transfer function on axis: the 3D probe showed large fluctuations in the digitized strength, while the 1D probe output is stable and reproducible.

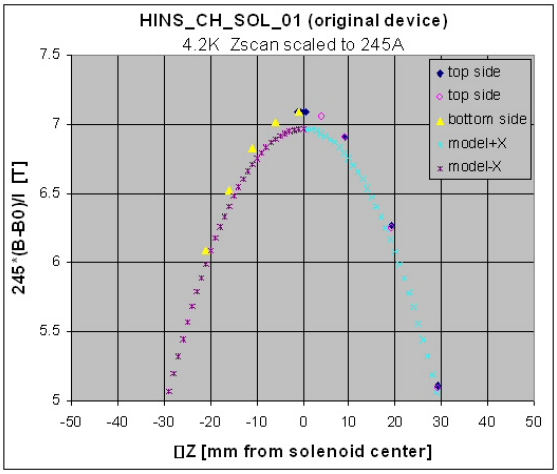

Figure 10. Comparison of measured and predicted central field strength, scaled to the predicted quench current of 245 A, in the peak field region.

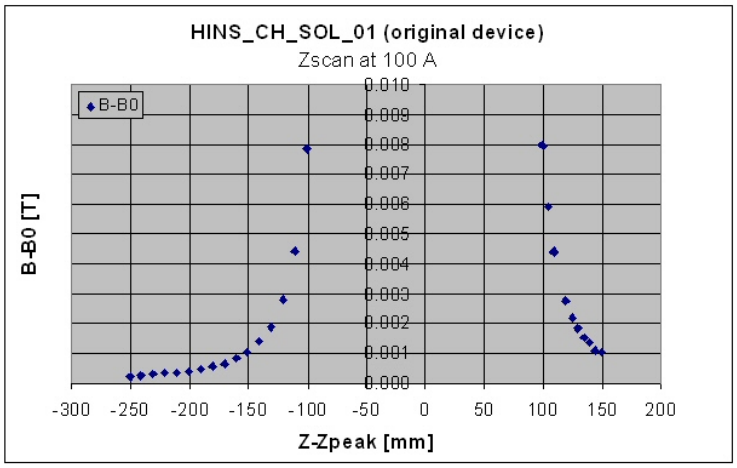

Figure 11. Field strength on axis at 100A at the extremes of the original lens.

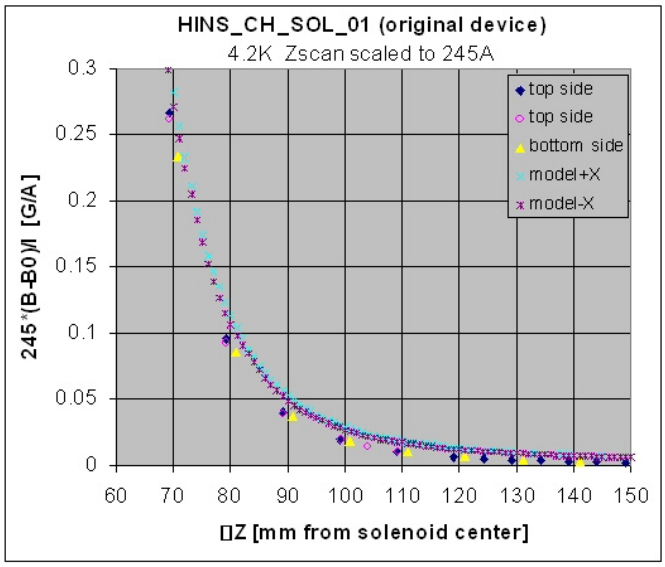

Figure 12. Comparison of measured and predicted central field strength, scaled to the predicted quench current of 245 A, at the extremes of the lens.

The rebuilt lens was tested again in February 2007, after extra power leads were added to the stand 3 top plate, and the buss arrangement was configured outside the Dewar. For each of the solenoid power configurations (Main Coil only, Bucked Coils only, Main+Bucked Coils), the field strength versus position was measured along the solenoid axis using Probe A. Figure 13 shows the strength profile on axis for the series combination of main and bucking coils. We find that the peak central field is about 4% stronger than the predicted value; this is consistent with the October 2006 transfer function, given the 1% difference in readback currents used. The field appears to be attenuated more efficiently than predicted around +/- 160 mm from the lens center, comparing Figure 14 to the calculation shown in Figure 3, and consistent with earlier measurements shown in Figure 12.

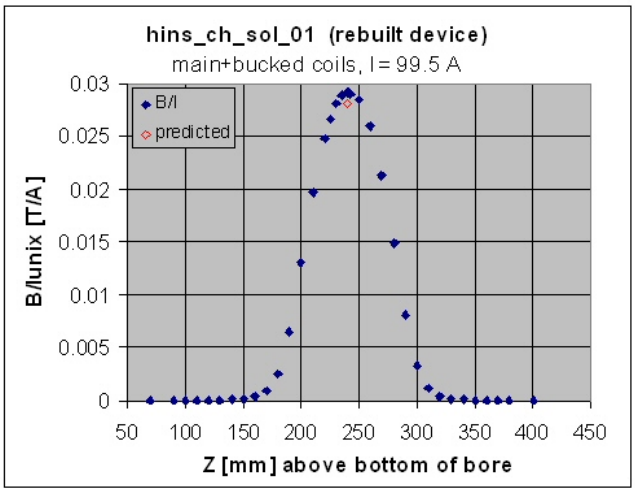

Figure 13. Field strength profile (normalized by current) along the rebuilt bucked coil solenoid axis, measured cold with 1D probe A.

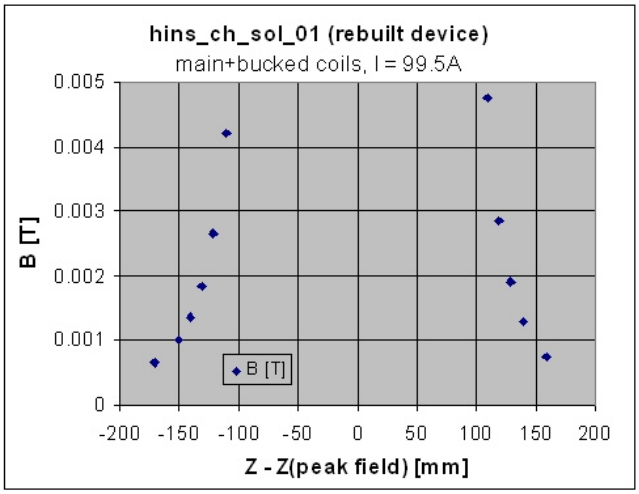

Figure 14. Field strength on axis at 100A at the extremes of the rebuilt lens.

The magnet underwent a thermal cycle for quench performance testing, after which a second round of magnetic measurements has been has been attempted, which appeared to be quite unsuccessful due to multiple complications with the measurement equipment and Hall probe and by lack of LHe to complete the test.

III. Conclusion

A long history of fabricating and quench testing the first prototype HINS focusing lens (without corrector dipoles) has shown that the choice of a preload and details of assembling the device are important in achieving reliable performance and easy training. In particular, it was important to incorporate a gap between the flux return body and flange, as suggested by 3D modeling, and to move the internal splices to a low field region. It was also shown that welding the LHe vessel, if done with some care, does not result in any degradation of lens performance. The quench current after training agrees with the prediction, and no retraining occurred after a thermal cycle to 300 K.

Magnetic measurements of the lens showed slightly higher peak coil fields, and the end field bucking is more efficient, than predicted by the model. Thus the magnetic properties are adequate. Studies to find the solenoid axis using a 3D Hall probe did not come to a quantitative conclusion due to problems with the probe readout; however, the qualitative results obtained suggest that one should be able to disentangle both position and angle offsets using this approach.

The tested lens meets all requirements and can be installed in a cryostat to be used as a focusing element in the HINS beam line. This lens was demonstrated to be self protecting and robust when the quench protection system failed, under the conditions that the power supply voltage is suitably limited and an adequate helium supply is maintained.

References

1. G. Davis, V.V. Kashikhin, T. Page, I. Terechkine, T. Wokas, Linac CH-Type Cavity Section Focusing Solenoid Cold Mass Design, FNAL TD note TD-06-020, FNAL, 2006.
2. B. Wands, Summary of DTL Section Solenoid FEA, FNAL TD note TD-06-043, FNAL, 2006